# Thermal time constant of a terminating type MEMS microwave power sensor*

Xu Yinglin(许映林) and Liao Xiaoping(廖小平)†

*(Key Laboratory of MEMS of Ministry of Education, Southeast University, Nanjing 210096, China)*

**Abstract:** A terminating type MEMS microwave power sensor based on the Seebeck effect and compatible with the GaAs MMIC process is presented. An electrothermal model is introduced to simulate the thermal time constant. An analytical result, about 160 ms, of the thermal time constant from the non-stationary Fourier heat equations for the structure of the sensor is also given. The sensor measures the microwave power jumping from 15 to 20 dBm at a constant frequency 15 GHz, and the experimental thermal time constant result is 180 ms. The frequency is also changed from 20 to 10 GHz with a constant power 20 dBm, and the result is also 180 ms. Compared with the analytical and experimental results, the model is verified.

**Key words:** MEMS; thermal time constant; microwave power; electrothermal model
**DOI:** 10.1088/1674-4926/30/10/104006 **EEACC:** 2575; 8460

## 1. Introduction

Microwave power plays an important role in wireless applications and communication systems. A sensor with high sensitivity, which can measure power accurately and quickly, is needed. Up to now, several structures of microwave power sensors have been introduced[1−3]. These sensors employ the principle of the conversion of electric power to heat, which is then indirectly measured. In Ref. [4], a terminating type MEMS microwave power sensor based on the Seebeck effect and compatible with the GaAs MMIC process is presented. The sensor measured the microwave power from –20 to 20 dBm up to 20 GHz. The sensitivity of the sensor is 0.27 mV/mW at 20 GHz, and the input return loss is less than –26 dB over the entire experiment frequency range. A most important characteristic of the thermoelectric power sensor is the thermal time constant. This parameter determines the transient response of the sensor when changing input power. Until now, there has been no published literature that discusses the thermal time constant of this kind of sensor in detail. In Refs. [5, 6], capacitance was used to model the thermal capacitance, and some simulation results were given. In Ref. [4], an electrothermal model is introduced to simulate the heat transfer behavior and temperature distribution. In this work, capacitance is added to the model in Ref. [4] and the simulation result of the thermal time constant is given. Compared with the analytical and experimental results, the model is verified.

## 2. Principle and model

The structure of the microwave sensor is shown in Fig. 1. A CPW feeds the microwave signal to the sensor. The CPW is designed to have a characteristic impedance of 50 Ω. It is terminated with resistive loads, which are matched to the characteristic impedance. The loads absorb the microwave power and convert it into heat. The resulting temperature increase of the loads is detected by the integrated thermocouples, which generate a DC voltage based on the Seebeck effect. The output voltage is proportional to the microwave power.

The CPW was made of a 2 $\mu$m thick gold layer. The thermopiles consisted of gold and $n^+$ GaAs. The gold strips of the

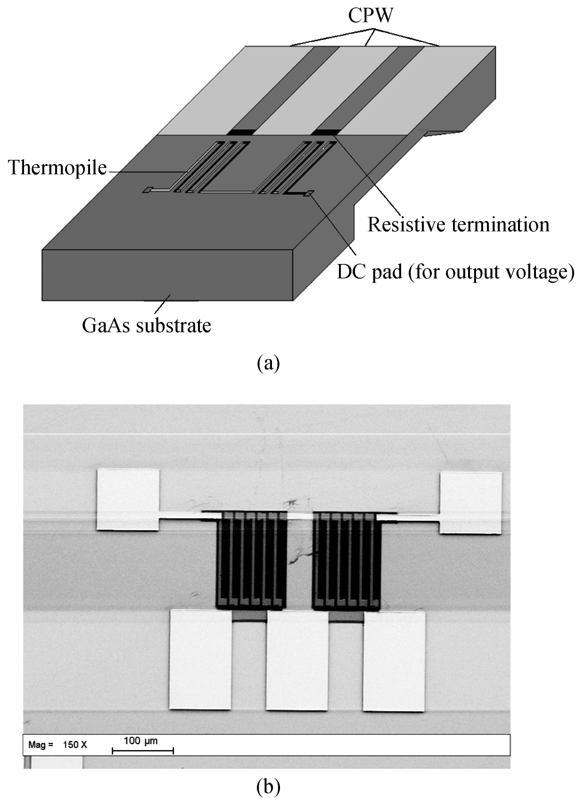


(a)

(b)

Fig. 1. (a) Schematic view of the microwave power sensor; (b) SEM photo of the microwave power sensor.

* Project supported by the National Natural Science Foundation of China (No. 60676043) and the National High Technology Research and Development Program of China (No. 2007AA04Z328).

† Corresponding author. Email: xpliao@seu.edu.cn

Received 16 March 2009, revised manuscript received 12 May 2009 

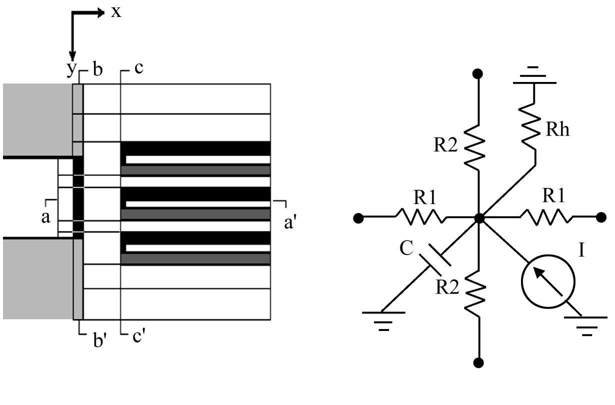


(a) (b)

Fig. 2. (a) Schematic view of the microwave power sensor; (b) Equivalent electrical circuit including convection, conduction, and heat generation.

thermopiles were made by the sputtering of a 0.3 $\mu$m thick gold layer, and the n$^+$ GaAs was made from a 0.25 $\mu$m thick epitaxial layer. By using a lift-off process through depositing of a TaN layer, matched loads were made with a square resistance of 25 Ω/□. The Seebeck coefficient of each thermocouple is 100 $\mu$V/K. A microphotograph of the microwave power sensor is shown in Fig. 1(b).

As described in Ref. [7], the 2D layout of the sensor is further subdivided into smaller elements, as shown in Fig. 2(a). Each element is then represented as the equivalent circuit in Fig. 2(b). The conductive transfer is represented by a thermal resistor,

$$R_{1,2} = l/\lambda A, \tag{1}$$

where $l$ is the length, $\lambda$ is the thermal conductivity, and $A$ is the cross section. The convective resistor is

$$R_{\rm h} = 1/hA_{\rm s}, \tag{2}$$

where $h$ is the heat-transfer coefficient, and $A_{\rm s}$ this time is the surface area. The thermal capacitance is

$$C = \rho c V, \tag{3}$$

where $\rho$, $c$, and $V$ are the density, specific heat capacity and volume of each element, respectively. The symbol for ground in Fig. 2(b) represents the ambient temperature, i.e., 300 K in this paper.

A cross-sectional view of the microwave sensor is shown in Fig. 3. The symbols $d_1$, $d_2$, and $d_3$ are the thicknesses of the resistive load, the thermocouple, and the GaAs substrate, respectively. $l_1$ is the width of the resistive load. $l_2$ is the distance between the hot junction and the load. $l_3$ is the length of the thermocouple.

Because the 3D structure is treated as 2D in the layout plane, the thermopile and the substrate should be regarded as one material. The same holds true for the resistive load and the substrate. In this work, some equivalent quantities used in Ref. [8, 9] are introduced. $\lambda_{\rm e1}$, $\rho_{\rm e1}$ and $c_{\rm e1}$ are the equivalent thermal conductivity, equivalent density and equivalent specific heat capacity of the resistive load and the substrate, while

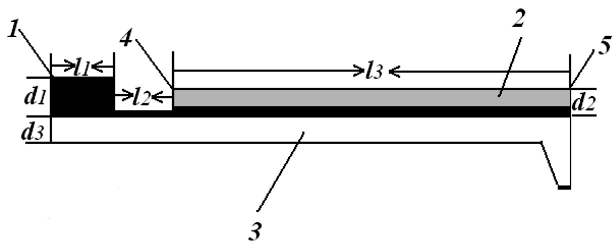


Fig. 3. Cross-sectional view of the microwave sensor. 1: Resistive load; 2: Thermocouple; 3: GaAs substrate; 4: Hot junction; 5: Cold junction.

$\lambda_{\rm e2}$, $\rho_{\rm e2}$ and $c_{\rm e2}$ denote the equivalent thermal conductivity, equivalent density and equivalent specific heat capacity of the thermopile and the substrate. They can be defined as

$$\lambda_{\rm e1} = \frac{\lambda_1 d_1 + \lambda_3 d_3}{d_1 + d_3}, \tag{4}$$

$$\lambda_{\rm e2} = \frac{\lambda_3 d_3 + \lambda_2 \frac{d_2}{2}}{d_{\rm e}} = \frac{\lambda_3 d_3 + \lambda_2 \frac{d_2}{2}}{d_3 + \frac{d_2}{2}}, \tag{5}$$

$$\lambda_2 = \frac{\lambda_{\rm n} + \lambda_{\rm p}}{2}, \tag{6}$$

$$\rho_{\rm e1} = \frac{\rho_1 d_1 + \rho_3 d_3}{d_1 + d_3}, \tag{7}$$

$$\rho_{\rm e2} = \frac{\rho_3 d_3 + \rho_2 \frac{d_2}{2}}{d_{\rm e}} = \frac{\rho_3 d_3 + \rho_2 \frac{d_2}{2}}{d_3 + \frac{d_2}{2}}, \tag{8}$$

$$\rho_2 = \frac{\rho_{\rm n} + \rho_{\rm p}}{2}, \tag{9}$$

$$c_{\rm e1} = \frac{c_1 d_1 + c_3 d_3}{d_1 + d_3}, \tag{10}$$

$$c_{\rm e2} = \frac{c_3 d_3 + c_2 \frac{d_2}{2}}{d_{\rm e}} = \frac{c_3 d_3 + c_2 \frac{d_2}{2}}{d_3 + \frac{d_2}{2}}, \tag{11}$$

$$c_2 = \frac{c_{\rm n} + c_{\rm p}}{2}, \tag{12}$$

$$\varepsilon_{\rm e} = \frac{\varepsilon_{\rm s} + \varepsilon_2}{2}, \tag{13}$$

$$\varepsilon_2 = \frac{\varepsilon_{\rm n} + \varepsilon_{\rm p}}{2}, \tag{14}$$

where $d_{\rm e}$ is the equivalent thickness of the thermopile and the substrate, and $\lambda_2$, $\rho_2$ and $c_2$ are the average thermal conductivity, average density and average specific heat capacity of the thermocouple with index $n$ and $p$ denoting the thermal conductivity of the positive and negative conductors of the thermocouple, respectively. By the same method, $\varepsilon_2$ is the average emissivity of the thermocouple.

Au and GaAs were chosen as the materials for the positive and negative conductors of the thermoelectric transducer, respectively. The following parameter values of the microwave power sensor were chosen: $\lambda_1$ = 34.7 W/(m·K), $\rho_1$ = 14360 kg/m$^3$, $c_1$ = 691 J/(kg·K), $l_1$ = 14.5 $\mu$m and $d_1$ = 2 $\mu$m; $\lambda_3$ = 46 W/(m·K), $\rho_3$ = 5320 kg/m$^3$, $c_3$ = 350 J/(kg·K), and

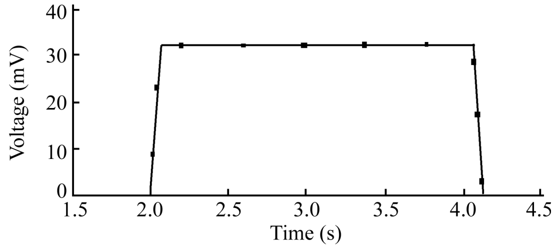


Fig. 4. Simulation result of thermal time constant.

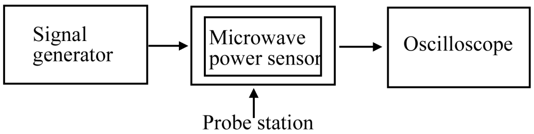


Fig. 5. Schematic of measurement.

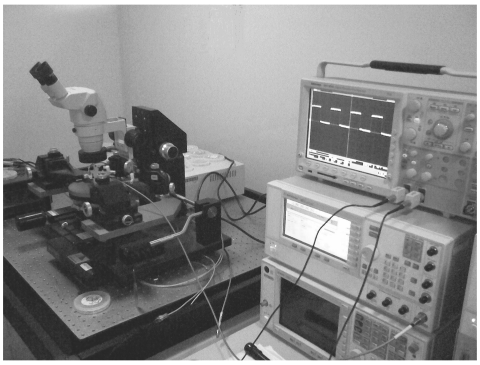

Fig. 6. Photo of measurement platform.

$d_3 = 10\,\mu$m; $\lambda_p$ = 315 W/(m·K), $\rho_p$ = 19300 kg/m$^3$, $c_p$ = 130 J/(kg·K), $l_3$ = 100 $\mu$m and $d_2$ = 0.25 $\mu$m; $\lambda_n$ = 46 W/(m·K), $\rho_n$ = 5320 kg/m$^3$ and $c_n$ = 350 J/(kg·K).

For the simulation, the constant current source jumped from 0 to 100 mA, equal to an input microwave power from 0 to 20 dBm for the sensor. The simulation result is shown in Fig. 4 and the thermal time constant is around 100 ms.

The analytical result of the thermal time constant from the non-stationary Fourier heat equations for the structure of the sensor is

$$\tau = \frac{1}{A_0} = \frac{1}{\dfrac{\pi^2}{4l^2}\dfrac{\lambda_e}{\rho_e c_e} + \dfrac{H}{\rho_e c_e d_e}}, \tag{15}$$

where $H = 2h + 4\sigma_b(\varepsilon_e + \varepsilon_2)T_0^3$ . The parameters are $\sigma_b$ = 5.67 × 10$^{-8}$ W/(m$^2$·K$^4$), $\varepsilon_n$ = 0.3, $\varepsilon_p$ = 0.02, $\varepsilon_s$ = 0.3, $T_0$ = 300 K, and $h$ = 1 W/(m$^2$·K). The numerical result is about 160 ms.

## 3. Experimental results

Measurements were performed using an Agilent E8257D PSG analog signal generator, a Tektronix DPO 4032 digital phosphor oscilloscope, and a Cascade Microtech 1200 probe station for contacting the sensor. The schematic of measurement is shown in Fig. 5. The microwave signal from a signal generator is sent to the microwave power sensor, and the output DC voltage is recorded by an oscilloscope. A photo of the measurement platform is given in Fig. 6.

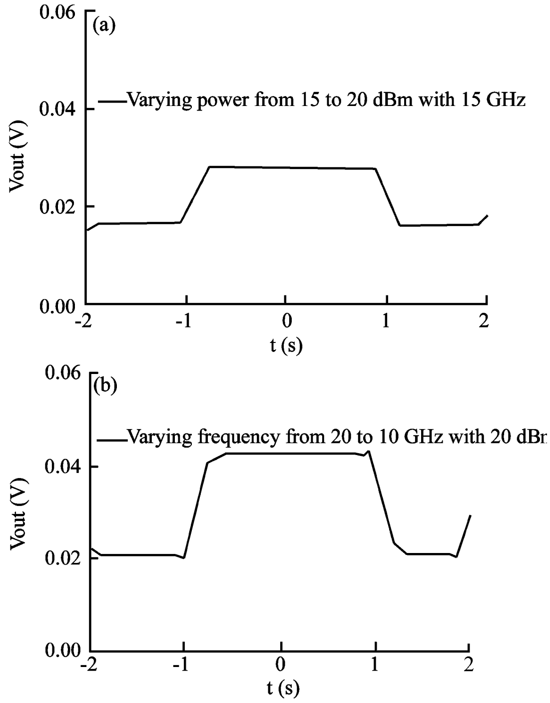


Fig. 7. Thermal time constant with different input conditions: (a) Varying power; (b) Varying frequency.

The relationship between output voltage and time can be seen in Fig. 7. Microwave power varying from 15 to 20 dBm at a constant frequency 15 GHz was applied in Fig. 7(a), while microwave frequency varying from 20 to 10 GHz with a constant power 20 dBm was applied in Fig. 7(b). The thermal time constants under different input conditions were identical, about 180 ms at the rising edge and 170 ms at the falling edge in both figures. Compared with the analytical and experimental results, they also present the same magnitude although there are some differences between them, and the model's accuracy is verified.

## 4. Conclusion

A thermal time constant model of a terminating type MEMS microwave power sensor is presented in this paper. Analytical and experimental results are also given. They are 160 ms and 180 ms, respectively. Compared with the analytical and experimental results, the model result is lower, at 100 ms. Considering the measurement instruments' response time, all the results present the same magnitude and the model's accuracy is verified.

## References

[1] Milanovic V, Gaitan M, Bowen E D, et al. Thermoelectric power sensor for microwave applications by commercial CMOS fabrication. IEEE Electron Device Lett, 1997, 18(9): 450

[2] Milanovic V, Gaitan M, Bowen E D, et al. Implementation of thermoelectric microwave power sensors in CMOS technology. IEEE International Symposium on Circuits and Systems, 1997, 4: 2753

[3] Milanovic V, Gaitan M, Zaghloul M E. Micromachined thermocouple microwave detector in CMOS technology. IEEE 39th Midwest Symposium on Circuits and Systems, 1996, 1: 273

[4] Xu Y L, Liao X P. Design and fabrication of a terminating type MEMS microwave power sensor. Journal of Semiconductors, 2009, 30(4): 044010

[5] Jia T H, Loc V Q. A rational formulation of thermal circuit models for electrothermal simulation-part I: finite element method. IEEE Trans Circuits Syst I: Fundamental Theory and Applications, 1996, 43(9): 721

[6] Charlot B, Mir S, Cota E F, et al. Fault modeling of suspended thermal MEMS. Proceedings of International Test Conference, 1999: 319

[7] Swart N R, Nathan A. Flow-rate microsensor modeling and optimization using SPICE. Sensors and Actuators A, 1992, 34: 109

[8] Kozlov A G. Optimization of thin-film thermoelectric radiation sensor with comb thermoelectric transducer. Sensors and Actuators A, 1999, 75: 139

[9] Kozlov A G. Optimization of thin-film thermoelectric radiation sensor with separate disposition of absorbing layer and comb thermoelectric transducer. Sensors and Actuators A, 2000, 84: 259